JOURNAL OF APPLIED ELECTROCHEMISTRY 5 (1975) 187–195

High oxide ion conduction in sintered oxides of the system Bi_2O_3-Y_2O_3

T, TAKAHASHI, H. IWAHARA, T. ARAO

Department of Applied Chemistry, Faculty of Engineering, Nagoya University, Nagoya, Japan

Received 6 August 1973

The ionic conduction in sintered Bi_2O_3–Y_2O_3 was investigated by measuring the conductivity and the emf of an oxygen concentration cell using the specimen tablet as electrolyte.

The face centred cubic phase in this system was found to show high oxide ion conduction accompanied by a little electronic conduction when exposed to air. This phase was stable with a composition of 25 ~ 43 mol % Y_2O_3 over a wide range of temperatures, and the oxide ion conductivity increased with decrease in Y_2O_3. The conductivities of $(Bi_2O_3)_{0.75}(Y_2O_3)_{0.25}$ were $1{\cdot}6 \times 10^{-1}\,\Omega^{-1}\,cm^{-1}$ at 700°C and $1{\cdot}2 \times 10^{-2}\,\Omega^{-1}\,cm^{-1}$ at 500°C values which are many times higher than those of stabilized zirconia $(ZrO_2)_{0.90}(Y_2O_3)_{0.10}$ at corresponding temperatures. Specimens containing less than 25 mol % Y_2O_3 showed a phase transition at 700 ~ 580°C and the conductivities decreased remarkably below these temperatures. High oxide ion conduction in the fcc phase is attributed to the migration of oxide ion vacancies which were present in an appreciable amount.

1. Introduction

As previously reported by the present authors [1, 2], sintered oxides of the system Bi_2O_3–SrO, Bi_2O_3–CaO, Bi_3O_2–La_2O_3 and Bi_2O_3–WO_3 were found to be high oxide ion conductors in certain ranges of composition, the conductivities of which were much higher than those of conventional stabilized zirconias at corresponding temperatures.

Of these materials, the sintered system Bi_2O_3–WO_3 has the highest conductivity; in particular $3Bi_2O_3WO_3$ and its solid solution are the highest oxide ion conductors known over a wide temperature range up to 850°C. They have a face centered cubic structure which corresponds to that of a high temperature modification (above 730°C) of pure Bi_2O_3 (δ-phase). The crystal structure of δ-Bi_2O_3 is of the defect fluorite-type [3, 4] having a large number of vacant sites in the oxide ion sub-lattice. The high electrical conduction is attributed to the migration of the oxide ion through the vacancies [1, 5, 6]. The temperature range over which this crystal structure is stable is, however, rather narrow [3] (730 ~ 825°C mp), and electronic conduction predominates below 730°C where the monoclinic structure (α-phase) is stable [1, 2, 7]. High oxide ion conduction in $3Bi_2O_3$–WO_3 and its solid solution at relatively low temperatures is considered also to be due to the same mechanism, since an appreciable number of oxide ion vacancies is considered to be present in these materials whose crystal structure is stable over a wide range below 730°C [2].

R. K. Datta *et al.* [8] reported that in the system Bi_2O_3–Y_2O_3 a compound $3Bi_2O_3Y_2O_3$ and the solid solution around it had the fcc phase, the crystal structure of which was related to the defect fluorite-type stable over a wide range of temperatures. The present authors have also observed a fcc phase in the binary system based on Bi_2O_3 and that it exhibits an extremely high oxide ion conductivity over a wide temperature range. In the present paper, the results of the investigation on ionic conduction in the system Bi_2O_3–Y_2O_3 are described. As attention has been mainly centred on high oxide ion conduction in the fcc phase of this system, the complex phase relationships in relatively low (< 10 mol % Y_2O_3) or high (> 50 mol % Y_2O_3) content of Y_2O_3 have also been roughly examined.

* Subscripts are mole fractions.

Table 1. Sintering temperature

Composition x in $(Bi_2O_3)_{1-x}(Y_2O_3)_x$	*Temperature* (°C)
0.00	750
0·05 ~ 0·09	810
0·10 ~ 0·20	850
0·225 ~ 0·30	870
0·33 ~ 0·40	910
0·425 ~ 0·55	970
0·60	1000

$x \times 100 =$ mol %.

2. Experimental

2.1. *Preparation of the sintered oxides*

The raw materials were yttrium sesquioxide (99·99%) and bismuth sesquioxide obtained by the thermal decomposition of bismuth nitrate (JIS; special grade) at 700°C for 2 h. The powders were mixed and calcined at 750 ~ 800°C for 10 h in air, then finely ground and pressed into rods (4 ~ 6 × 8 ~ 12 mm) or tablets (13 × 2 ~ 3 mm) under 2·7 ~ 4·0 ton cm^{-2} and sintered in air for 10 h. As shown in Table 1, the sintering temperature was changed according to the composition; the best sintered state was obtained at temperatures somewhat below any particular melting point.

X-ray diffraction was carried out using CuK α radiation. Densities of the powdered specimens were determined by the standard pykometric method using *n*-butanol at 25°C. Thermogravimetric analyses were performed at a heating rate of 8°C min^{-1} up to 900° at which the temperature was held for 3 h. The differential thermal analysis data were compared with the conductivity to observe the phase transformation.

2.2. *Measurement of ionic conduction*

The ionic conduction in the specimen was examined by measuring the electrical conductivity and the emf of an oxygen concentration cell.

Platinum powder paste was smeared on the both ends of the prepared sintered rods and baked to serve as the electrodes. A measuring frequency of 10 KHz was used, in the vicinity of which the dependence of conductivity on frequency was negligibly small.

If the conduction in the specimen is purely ionic, the emf E_0 of the cell:

$$O_2(P_{O_2,a}), Pt \mid \text{specimen tablet} \mid Pt, O_2(P_{O_2,c}) \quad (1)$$

is given by Equation 2:

$$E_0 = \frac{RT}{4F} \ln P_{O_2,c}/P_{O_2,a} \quad (2)$$

where R, T and F have their usual meanings. In the mixed conductor, in which the conduction is both ionic and electronic, the emf is lowered to some extent, and the ratio of the ionic conductivity σ_i to the total value $\sigma = \sigma_i + \sigma_e$ (where σ_e is the electronic conductivity), that is, the ion transference number t_i, can be determined as a ratio of the measured emf E to the theoretical value E_0:

$$t_i = \frac{\sigma_i}{\sigma_i + \sigma_e} = \frac{E}{E_0}, \quad (3)$$

when the reversibility of the electrode reaction is good.

Air, free from H_2O and CO_2, was usually used as anode gas, and pure oxygen at 1 atm was used as the cathode gas. The procedure and apparatus for these measurements were similar to those described previously [1, 10].

3. Results

3.1. *Specimens prepared*

The porosities of the sintered specimens were less than 10% in the composition range between 5 and 40 mol % Y_2O_3. They were somewhat larger in the specimens of higher content of Y_2O_3 though the open pores to allow the penetration of gas were not recognized. The colour of the sintered materials changed from reddish orange to pale orange as the content of Y_2O_3 increased.

Fig. 1 shows the X-ray diffraction patterns of the specimens which were cooled from sintering temperatures (above 800°C) to room temperature for 3 h. The single phase of face centred cubic type structure which was related to the diffraction pattern of the high temperature modification of pure Bi_2O_3 was observed in the samples containing 10 ~ 40 mol % Y_2O_3. As represented in Fig. 2, the lattice constants of these specimens decreased with

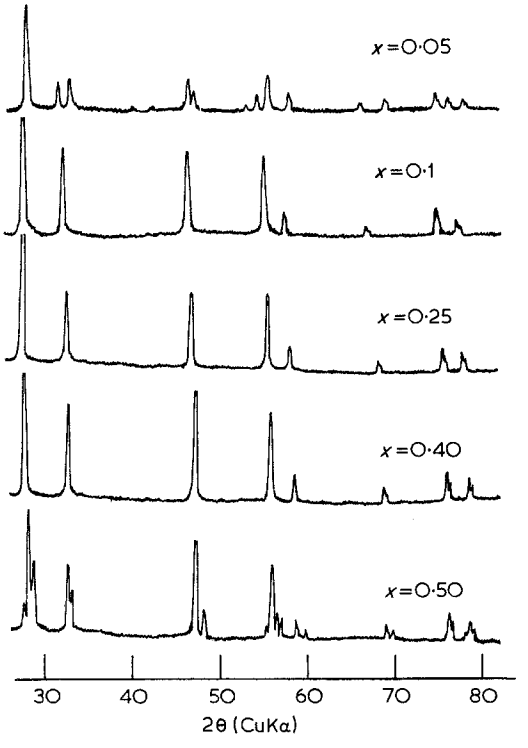

Fig. 1. X-ray diffraction patterns of $(Bi_2O_3)_{1-x}(Y_2O_3)_x$ cooled from sintering temperature (above 800°C) to room temperature for 3 h.

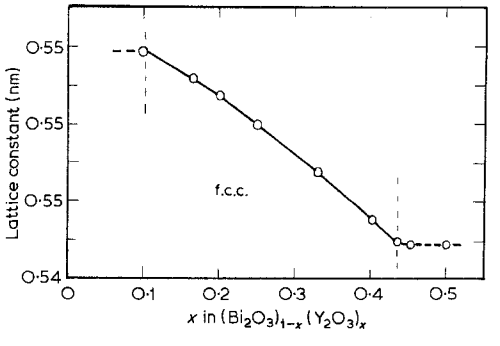

Fig. 2. Lattice constant of fcc phase of the specimens cooled from sintering temperature (above 800°C) to room temperature for 3 h.

increase in the content of Y_2O_3. Vegard's rule almost held in the composition range from 10–43·5 mol % Y_2O_3 though some curvature was observed. This implies that the system Bi_2O_3–Y_2O_3 forms a solid solution of cubic type over a wide range of composition, as pointed out by Datta *et al.* In their work, the lattice constants were reported to have a maximum value at 25 mol % Y_2O_3. Our result shows, however, a monotonic decrease in lattice constant with increasing content of Y_2O_3 in the composition range 10 ~ 43 mol %.

Specimens containing less than 10 mol % contained the tetragonal phase, and those containing more than 43 mol % Y_2O_3, the mixed phase of face centred cubic and body centred cubic structure, these studies were however not carried out in detail.

3.2. *Conductivity of the sintered specimens*

The conductivities of the sintered Bi_2O_3–Y_2O_3 system measured in air are shown in Fig. 3 as an Arrhenius plot. As previously reported [1, 2], the conductivity of pure Bi_2O_3 is relatively low below 730°C, and the sudden increase in conductivity appears at this temperature which corresponds to the transformation from monoclinic to cubic phase.

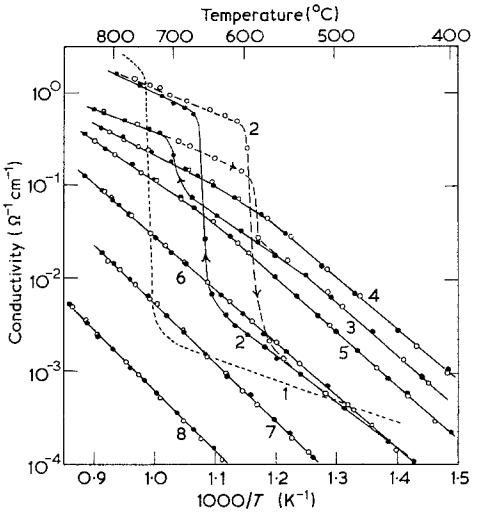

Fig. 3. Conductivity of $(Bi_2O_3)_{1-x}(Y_2O_3)_x$ in air. The values for x ($x \times 100$ = mol %) are: 1 - 0; 2 - 0·05; 3 - 0·20; 4 - 0·25; 5 - 0·33; 6 - 0·425; 7 - 0·50; 8 - 0·60.

However, the sintered samples containing more than 25 mol % Y_2O_3 showed no jump in conductivity in the whole range of temperature examined. The conductivities of these specimens below 700°C were higher than those of pure Bi_2O_3 over a wide range of composition, while the values in the high temperature region were lower than those of pure Bi_2O_3.

Specimen containing less than 20 mol % Y_2O_3 gave a sudden increase in conductivity at 580 ~ 700°C,

the degree of which grew remarkably as the Y_2O_3 content decreased. Marked thermal hysteresis in conductivity between the heating and the cooling process was observed in these samples. As indicated in Fig. 3 with a dotted line for $(Bi_2O_3)_{0.95}(Y_2O_3)_{0.05}$ and $(Bi_2O_3)_{0.80}(Y_2O_3)_{0.20}$, the conductivity during the cooling process decreased along the extrapolated line of the conductivity curve in the higher temperature range, and dropped rapidly at temperatures lower by 50 ~ 100°C than the temperature at which the conductivity jumped during the heating process.

3.3. *The relation between conductivity and the phase*

The jump in conductivity suggests that the phase transition is occurring at these temperatures, although previous investigators did not give such information in the composition range from 10 to about 30 mol % Y_2O_3. The X-ray diffraction patterns of slowly cooled samples differed from those of the fcc single phase indicating that the transformation was included as represented in Fig. 4 for $(Bi_2O_3)_{0.833}(Y_2O_3)_{0.167}$ and $(Bi_2O_3)_{0.80}(Y_2O_3)_{0.20}$. Specimens containing more than 25 mol % Y_2O_3 showed no change in X-ray diffraction pattern even after annealing at 500°C for 24 h and cooled slowly to room temperature.

Differential thermal analysis showed exothermic peaks at the temperatures of the jump in conductivity, whereas no thermal change was observed in the specimens containing more than 25 mol % Y_2O_3. As shown in Fig. 5, the exothermic transformation temperature corresponds closely to the temperature at which the increase in conductivity takes place. This means that the latter is due to the transformation to the fcc single phase. As shown in Fig. 3, this phase is highly conductive when compared to the other phases, though its conductivity decreases with increasing content of Y_2O_3.

As a result, in the specimens containing more than 25 mol % Y_2O_3, the fcc single phase is stable over a wide temperature range, while, in the region of poorer Y_2O_3 content, this phase is unstable below the temperatures indicated in Fig. 5. Correspondingly, sintered samples containing more than 25 mol % Y_2O_3 gave no discontinuous change in conductivity whereas with less than 25 mol % Y_2O_3 a discontinuous decrease in conductivity appears at a certain temperature. The conductivities

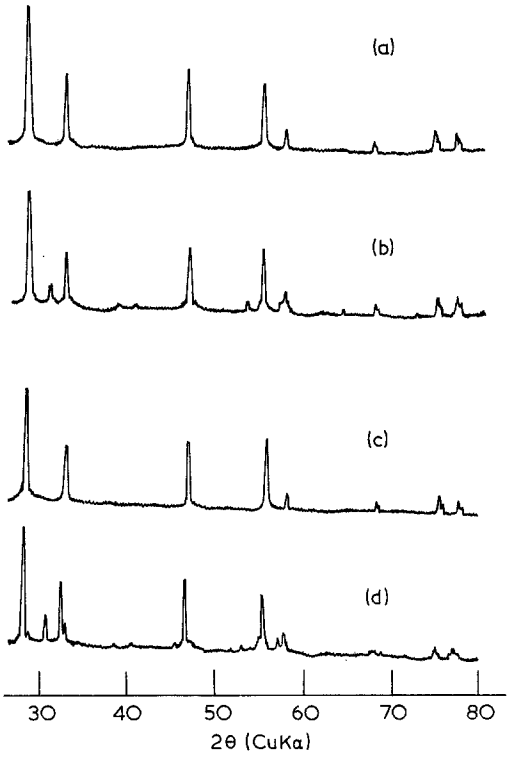

Fig. 4. Comparison of X-ray diffraction patterns between the rapid cooled and the annealed specimens.
(a) $(Bi_2O_3)_{0.833}(Y_2O_3)_{0.167}$ - cooled from 850°C to room temperature for 3 h.
(b) $(Bi_2O_3)_{0.833}(Y_2O_3)_{0.167}$ - annealed at 500°C for 24 h.
(c) $(Bi_2O_3)_{0.80}(Y_2O_3)_{0.20}$ - cooled from 850°C to room temperature for 3 h.
(d) $(Bi_2O_3)_{0.80}(Y_2O_3)_{0.20}$ - annealed at 500°C for 24 h.

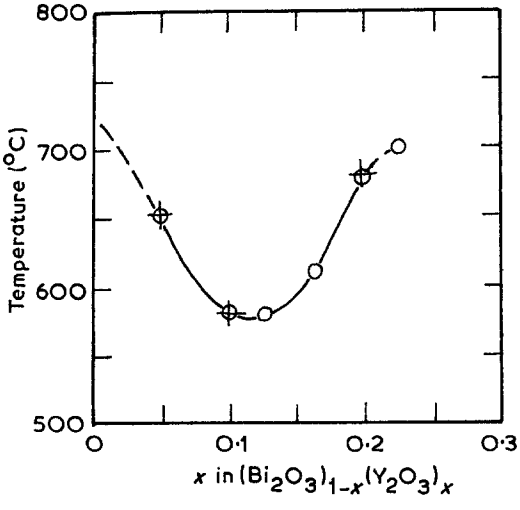

Fig. 5. Temperature of the jump in conductivity (o) and transformation temperature by D.T.A. (+).

of the former at lower temperatures are higher than those of the latter whilst the reverse holds at higher temperatures.

Table 2. Ratios of the measured emf E to the theoretical value E_0 of the following cell: O_2(0·21 atm), Pt | $(Bi_2O_3)_{1-x}(Y_2O_3)_x$ | Pt, O_2(1·0 atm)

x	E/E_0 550°C	600°C	700°C	800°C
0	0	0	0 0·97	0·97
0·05	0·85	0·90 0·97	0·98	0·99
0·10	1·00	0·97	0·97	0·98
0·20	–	0·89	0·94	0·98
0·25	0·98	0·96	0·97	0·98
0·33	–	0·99	0·98	0·98
0·425	0·98	0·95	0·95	0·96
0·50	–	0·93	0·90	0·90
0·60	–	0·31	0·50	0·64

The upper and lower figures in the same column represent the value during heating and cooling, respectively)
$x \times 100$ = mol%.

3.4. *Properties of conduction*

Table 2 shows the ratio of the measured emf to the theoretical value of the oxygen concentration cell using the sintered tablet as the electrolyte under the condition of $P_{O_2,a} = 0{\cdot}21$ and $P_{O_2,c} = 1{\cdot}0$ atm. As previously reported [1, 2], the emf of the cell using pure Bi_2O_3 could not be detected up to 730°C where it appeared suddenly and increased rapidly to the theoretical value as the temperature was raised. This is in accordance with temperature at which the jump in conductivity occurs and, therefore, the monoclinic-cubic transformation takes place.

In contrast specimens containing a certain amount of Y_2O_3 showed the emf even in the temperature range below 700°C indicating the existence of ionic conduction. The value of E/E_0 was greater than 0·9 in most cases, indicating that charge carriers in these oxides were mainly ions. Thermal hysteresis of the fraction E/E_0 was observed in specimens of extremely low content of Y_2O_3 such as $(Bi_2O_3)_{0{\cdot}95}(Y_2O_3)_{0{\cdot}05}$. As shown in Fig. 6, E/E_0 at low temperature was somewhat low suggesting that some electrons or electron holes took part in conduction, and at 670° a remarkable increase in E/E_0 was noted during the heating process, which had remained at around unity until 600°C during cooling and then decreased rapidly to the original value. The temperature at which E/E_0 changes corresponds to that at which the jump in conductivity takes place and, therefore, to the transition from tetragonal to cubic. In specimens containing more than 10 mol% Y_2O_3, the values of E/E_0 were higher than 0·9 over the whole temperature range examined, despite the fact that the jump in conductivity and, therefore, the phase transition, was observed in compositions less than 25 mol% Y_2O_3. Thus the electronic conduction of the low temperature phase is not so remarkable.

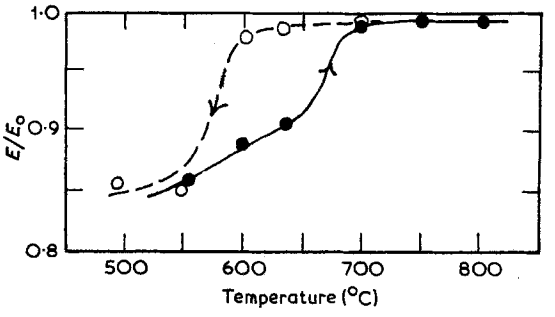

Fig. 6. E/E_0 of the following cell O_2(0·21 atm), Pt | $(Bi_2O_3)_{0{\cdot}95}(Y_2O_3)_{0{\cdot}05}$ | Pt, O_2 (1 atm).

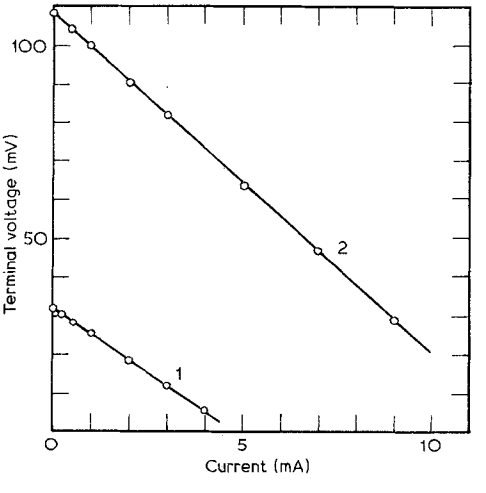

Fig. 7. Discharge curves of the following cell at 700°C. $O_2(P_{O_2,a})$, Pt | $(Bi_2O_3)_{0{\cdot}75}(Y_2O_3)_{0{\cdot}25}$ | Pt, O_2 (1 atm). Electrolyte thickness: 2·5 mm; Electrode area: 0·5 cm^2. 1: $P_{O_2,a} = 0{\cdot}21$ atm, 2: $P_{O_2,a} = 1{\cdot}30 \times 10^{-3}$ atm.

Considerably higher currents could be drawn continuously from these cells. Fig. 7 shows the

relation between the current density and the terminal voltage of the cell using $(Bi_2O_3)_{0.75}(Y_2O_3)_{0.25}$ as electrolyte under the conditions of $P_{O_2,a}$ = 0·21 and $1{\cdot}3 \times 10^{-3}$ atm, keeping $P_{O_2,c} = 1{\cdot}0$ atm at 700°C. The cell was stable and reproducible even after being short-circuited for a long time. These results indicate that the conducting ion should be the oxide ion as in sintered Bi_2O_3–WO_3 and Bi_2O_3–SrO. For, if the cations were charge carriers, considerable polarizations should arise because of the irreversibility of the electrode reaction, and a high stable current density could not then be drawn from the cell. Furthermore, by means of the method previously described [1], oxygen gas was detected at the anode without decomposition of the electrolyte when direct current was passed.

As a consequence, the conductivities shown in Fig. 3 are considered to be oxide ion conductivities in the composition range 10 ~ 50 mol % Y_2O_3. The oxide ion conductivities of these materials are remarkably high as compared to those of conventional oxide ion conductors such as the stabilized zirconias. Moreover, some exhibit the higher oxide ion conductivity at lower temperatures than those of previously reported systems such as Bi_2O_3–SrO and Bi_2O_3–WO_3. For example, the oxide ion conductivities of $(Bi_2O_3)_{0.75}(Y_2O_3)_{0.25}$ are $1{\cdot}6 \times 10^{-1}\ \Omega^{-1}\ cm^{-1}$ at 700°C, $8{\cdot}0 \times 10^{-2}\ \Omega^{-1}\ cm^{-1}$ at 600°C and $1{\cdot}2 \times 10^{-2}\ \Omega^{-1}\ cm^{-1}$ at 500°C, many times greater than those of $(ZrO_2)_{0.9}(Y_2O_2)_{0.1}$ at corresponding temperatures.

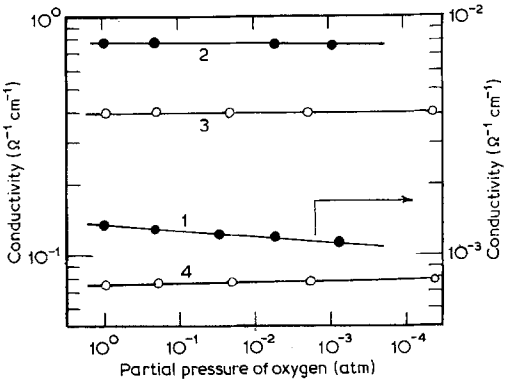

Fig. 8. Dependence of conductivities on oxygen partial pressure. 1 - $(Bi_2O_3)_{0.95}(Y_2O_3)_{0.05}$ at 550°C; 2 - $(Bi_2O_3)_{0.95}(Y_2O_3)_{0.05}$ at 700°C; 3 - $(Bi_2O_3)_{0.75}(Y_2O_3)_{0.25}$ at 600°C; 4 - $(Bi_2O_3)_{0.75}(Y_2O_3)_{0.25}$ at 800°C.

The existence of some electronic conduction in the specimen $(Bi_2O_3)_{0.95}(Y_2O_3)_{0.05}$ at low temperature was confirmed by the dependence of conductivity on oxygen partial pressure. As shown in Fig. 8, the conductivities of this material in the low temperature region decreased with decreasing partial pressure of oxygen, indicating that the electronic conduction was due to the electron hole (*p*-type) conduction, while the pressure dependence of the conductivities in the high temperature range where E/E_0 was nearly unity, was not recognized in the pressure range examined. In the specimens which showed no jump in both conductivity and E/E_0, the dependence of conductivity on the oxygen partial pressure was not seen over the whole temperature range studied, which suggested that the electronic conduction in this case was negligibly small, and that the true transference number of ion would be somewhat higher than those calculated from E/E_0, since a negligibly small electronic conduction could often cause the lowering of the emf appreciably when the polarization of the oxygen electrode was appreciable. In reducing atmospheres such as CO_2–CO, these materials tend to be reduced and to consequently have substantial *n*-type electronic conduction.

4. Discussion

From the results described, it is concluded that the fcc phase in the Bi_2O_3–Y_2O_3 system is a high oxide ion conductive phase like the Bi_2O_3–WO_3 system in which the composition region of the fcc phase is rather narrow at low temperatures compared with that in the former. Table 3 shows the values for activation energies and pre-exponential terms for the Arrhenius plots of the conductivity of the fcc phase taken from the data in Fig. 3. The activation energies in the high temperature region increased as the content of Y_2O_3 increased, whereas those in the low temperature range were almost constant.

In Fig. 9, the oxide ion conductivities in the Bi_2O_3–Y_2O_3 system were plotted against the content of Y_2O_3. In the high temperature region above 700°C where the fcc single phase is stable, the conductivities decrease monotonically with increase in the content of Y_2O_3. In this range, the logarithm of the conductivity versus the content of Y_2O_3 plot gives a straight line up to about 40 mol % Y_2O_3 where a knee appears because of the solubility

Table 3. Activation energies and pre-exponential terms for the Arrhenius plots of the conductivity of the fcc phase

x in $(Bi_2O_3)_{1-x}(Y_2O_3)_x$	*High temperature range* > 600°C		*Low temperature range* < 550°C	
	Pre-exponential term, Ω^{-1} cm^{-1}	*Activation energy, eV*	*Pre-exponential term,* Ω^{-1}cm^{-1}	*Activation energy, eV*
0·25	$4{\cdot}6 \times 10^2$	0·66	$1{\cdot}1 \times 10^5$	1·07
0·33	$1{\cdot}9 \times 10^3$	0·84	$4{\cdot}2 \times 10^4$	1·10
0·425	$1{\cdot}0 \times 10^4$	1·10	$1{\cdot}0 \times 10^4$	1·10

$x \times 100 =$ mol%.

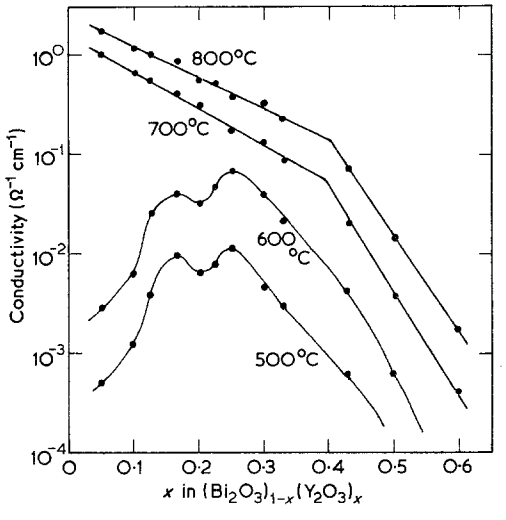

Fig. 9. Oxide ion conductivity of $(Bi_2O_3)_{1-x}(Y_2O_3)_x$ in air for various compositions.

limit of Y_2O_3 in the fcc single phase. The conductivity curves below 600°C have a maximum at the lower limit of the content of Y_2O_3 in the fcc phase. The fact that the oxide ion conductivity has a maximum value at the lower limit of the formation range of the solid solution has a parallel in the Bi_2O_3–WO_3 system as previously reported [2]. . This tendency is coincident with the general trend for stabilized zirconias that the composition giving the highest oxide ion conductivity lies at the lowest content of the second cation within the solid solution formation range. Consequently, $(Bi_2O_3)_{0{\cdot}75}(Y_2O_3)_{0{\cdot}25}$ might be the most desirable composition for practical use as an oxide ion conductor, since this had the lowest content of Y_2O_3 which caused no transformation and had the highest conductivity over a wide range of temperatures.

Another maximum of the conductivity curves which appeared in the composition range below 20 mol% Y_2O_3 has not been studied in detail.

High oxide ion conduction in the fcc phase is considered to relate to the oxide ion vacancies in the crystal as in the case of the conduction in δ-Bi_2O_3 and $3Bi_2O_3.WO_3$. The X-ray diffraction pattern of this phase resembles that of Bi_2O_3. Datta *et al.* described $3Bi_2O_3$–Y_2O_3 and its Bi_2O_3-rich side solid solutions as having two vacancies per unit cell of the defect fluorite-type lattice, that is the unit cell was described as $Bi_{4(1-x)}Y_{4x}O_6\square_2$, where □ represents an oxide ion vacancy and x was 0·1 ~ 0·25.

According to our experimental results, however, the fcc single phase containing less than 25 mol% Y_2O_3 was stable only above the temperature where the jump in conductivity took place, and the lattice constants decreased with increasing Y_2O_3 over a wide range up to $x = 0{\cdot}43$.

Theoretical densities of these materials have been calculated from the lattice constants obtained in the present experiment assuming the following three cases. (1) All cations occupy their normal sites in the fluorite-type lattice and two of eight oxide ions per unit cell are vacant, i.e. $Bi_{4(1-x)}Y_{4x}O_6\square_2$; (2) all cations and anions occupy their normal sites, respectively, and the above vacant sites are occupied by oxygen atoms or by ionized oxygen accompanied by electron holes, i.e. $Bi_{4(1-x)}Y_{4x}O_8$; (3) all Bi^{3+} ions occupy their normal sites and all Y^{3+} ions are situated at the interstitial sites, i.e. $Bi_4Y_{4x/(1-x)}O_{6/(1-x)}$.

In Fig. 10 the calculated densities for each model and the pyknometric densities measured are plotted against the content of Y_2O_3. The observed values were situated in the intermediate position between the curves for model 1 and 2 over the whole range of composition measured. This result seems to indicate that one of the two vacancies per unit cell of the

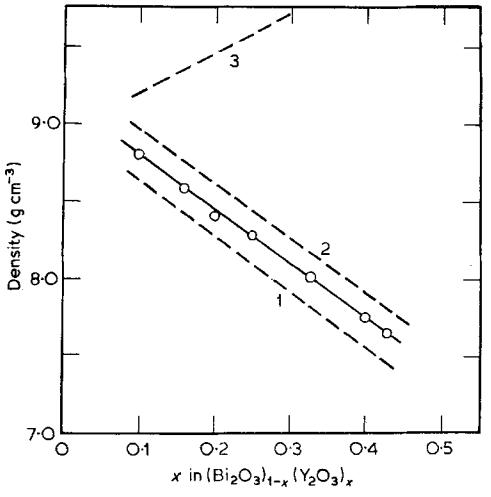

Fig. 10. Observed densities and calculated densities for various crystal models. 1 - for model 1 i.e. $Bi_{4(1-x)}Y_{4x}O_6\square_2$, 2 - for model 2 i.e. $Bi_{4(1-x)}Y_{4x}O_8$, 3 - for model 3 i.e. $Bi_4Y_{4x/(1-x)}O_6/_{(1-x)}$. The open circles represent measured densities.

model 1) is filled by excess oxide ion accompanied with two electron holes i.e.

$$\tfrac{1}{2}O_2 + \square \rightarrow O^{2-} + 2h^+ \qquad (4)$$

This explanation cannot be sustained for the following reason. If the excess oxide ions were formed according to Equation 4, an increase in the weight should occur during the solid state reaction of Bi_2O_3 and Y_2O_3 on heating in air. Thermogravimetric analysis of this reaction, however, showed negligible change in weight which indicated that the excess oxygen was absent in the crystal. In addition, if the excess of the oxide ions was present according to Equation 4, the conduction by electron holes would arise which was not found in these materials.

As a result, the penta-valent cations (Bi^{5+} or Y^{5+}) are considered not to be present and all cations remain in the tri-valent state. In such a case, it may be rational to consider that some of the cations are situated on interstitial sites such as $(\frac{1}{2}, \frac{1}{2}, \frac{1}{2})$ which have a relatively large space surrounded by eight nearest oxide ions in the fluorite-type lattice. As a consequence, the oxide ion vacancies described in model 1 would be partly filled by the oxide ions which arise from the charge compensation due to the interstitial tri-valent cations, that is,

$$3\square + 2(\ )_i + M_2O_3 \rightarrow 3O^{2-} + 2(M^{3+})_i. \qquad (5)$$

In such a model, the electronic conduction must be low, and, moreover, the densities of these materials are higher than those of the model 1 which correspond to the results of the present experiment. The available interstitial cation in this case would be Y^{3+} because its ionic radius is slightly smaller than that of Bi^{3+} (ionic radius; 0.092 nm for Y^{3+}, 0.096 nm for Bi^{3+}). The numbers of interstitial cations and oxide ion vacancies per unit cell in this model were estimated from observed densities to be 0·12 ~ 0·22 and 1·83 ~ 1·87, respectively.

5. Conclusions

Sintered oxide of the system Bi_2O_3–Y_2O_3 was found to give high oxide ion conduction on the Bi_2O_3-rich side. In particular, the fcc single phase in this system exhibited extremely high conductivities many times higher than those of the stabilized zirconias at corresponding temperatures. The electronic conduction in this phase was negligibly small under ambient atmospheres. The fcc phase in the composition range between 25 and 43 mol % Y_2O_3 was stable from room temperature to 850°C at least while, in the composition range less than 25 mol % Y_2O_3, it was unstable below the temperature at which the increase in conductivity took place. The oxide ion conductivities in the fcc phase increased with decreasing content of Y_2O_3. Consequently, $(Bi_2O_3)_{0.75}(Y_2O_3)_{0.25}$ has the most desirable composition in this system, since this shows no transformation and has the highest conductivity over a wide range of temperature.

High oxide ion conduction in the fcc phase was attributed to the migration of oxide ion vacancies since it was estimated from the density measurements that an appreciable amount of these were present.

References

[1] T. Takahashi, H. Iwahara and Y. Nagai, *J. Appl. Electrochem.* **2** (1972) 97.
[2] T. Takahashi and H. Iwahara, *J. Appl. Electrochem.* **3** (1973) 65.
[3] G. Gattow and D. Schutze, *Z. anorg. allg. Chem.* **328** (1964) 44.
[4] G. Gattow and H. Schroder, *Z. anorg. allg. Chem.* **318** (1962) 176.
[5] R. S. Sethi and H. C. Gaur, *Indian J. Chem.* **3** (1955) 177.
[6] M. G. Hapase and V. B. Tare, *Indian J. Pure Appl. Phys.* **5** (1967) 401.

[7] C. N. R. Rao, G. V. Subba Rao and S. Ramdas, *J. Phys. Chem.* 73 (1969) 672.
[8] R. K. Datta and J. P. Meehan, *Z. allg. Chem.* **383** (1971) 328.
[9] C. Wagner, *Z. Phys. Chem.* **21** (1925) 25.
[10] T. Takahashi and H. Iwahara, *Energy Conversion* **11** (1971) 105.